Effects of Surrounding Buildings on Air Patterns and Turbulence in Two Naturally Ventilated Mediterranean Greenhouses Using Tri-Sonic Anemometry

A. López, D. L. Valera, F. D. Molina-Aiz, A. Peña

Abstract. *The aim of the present study is to increase the available information concerning the influence of surrounding buildings on air patterns and turbulence characteristics of the ventilation airflow in greenhouses. With a view to evaluating the possible effect of different obstacles close to greenhouse vents, sonic anemometry has been used. At the side opening, the airflow was mainly horizontal, while at the roof vent it was upward or downward. The vicinity of obstacles to the greenhouse side openings reduced the incoming mean flow up to 79% and increased turbulence. Larger ventilation rates were observed for the leeward roof vent, since the wind impacts directly with the windward side opening without obstacles, with a maximum of 31.6 air exchanges per hour. However, when the roof vent is on the windward side, the wind is partially blocked by another similar greenhouse located upwind, as the outside air enters through the roof vent and exits through the two side openings. In this situation, the maximum ventilation rate observed was 14.5 air exchanges per hour. Natural ventilation was more effective in eliminating heat from the part of the greenhouse with a crop when the air entered through the side openings and exited through the roof vent. In this case, the ventilation efficiency for temperature (η_T) was greater than 1. The maximum turbulence levels were associated with low air speeds and were observed mainly at the points located close to the side openings influenced by surrounding buildings. The turbulent energy levels of the airflow were higher at the windward openings without obstacles.*

Keywords. *Greenhouse, Sonic anemometry, Turbulence, Insect-proof screens, Ventilation.*

Almería province (Spain) is one of Europe's leading areas of horticultural production, and this sector is the driving force behind the province's economy. The development and increase in agricultural activity over recent decades has involved the proliferation of greenhouses, which at present cover a surface area of approximately 30,000 ha. Most of these greenhouses are located in coastal areas of the province. This high concentration of productive units means that there is very little space between greenhouses, in many cases less than 1 m. This proximity means that air does not flow freely through the side vents of the greenhouse (Katsoulas et al., 2006; Kittas et al., 2008), which can be a serious drawback in summer, when cooling is essential, requiring the use of side and roof vents to facilitate more efficient ventilation (Montero et al., 2001; Pérez-Parral et al., 2004; Katsoulas et al., 2006).

The main driving forces of ventilation for a greenhouse equipped with both roof and side openings are caused by a combination of pressure differences induced by the following effects (Boulard and Baille, 1995; Kittas et al., 1997; Baptista et al., 1999): the static wind effect due to the mean component of the wind velocity, which induces pressure differences (side wall effect) between the side and the roof openings (Bruce, 1978) and pressure differences between the windward and leeward parts of the greenhouse (Boulard et al., 1996); the buoyancy forces (also called stack or chimney effect) generating a vertical distribution of pressures between the side and roof openings (Bruce, 1982); and the turbulent effect of the wind, generated by pressure fluctuations of the wind velocity along and across the greenhouse openings (Boulard and Baille, 1995; Boulard et al., 1996).

The greenhouse ventilation rate is affected not only by the wind but also by the buoyancy generated by the difference between the inside and outside air temperatures (ΔT_{io}). Papadakis et al. (1996) pointed out that the buoyancy-driven ventilation was fundamental, particularly for air speeds less than 1.8 m s^{-1}. For greenhouses with side and roof vents, Kittas et al. (1997) established that the chimney effect is important when $u_o/\Delta T_{io}^{0.5} < 1$, where u_o is the wind velocity, while Bot (1983) set this limit at 0.3.

To date, most studies on natural ventilation have been based on estimations of a total exchange rate of air using gas tracer techniques (Bot, 1983; Fernandez and Bailey, 1992; Boulard and Draoui, 1995; Kittas et al., 1995; Papadakis et al., 1996; Kittas et al., 1996; Baptista et al., 1999; Kittas et al., 2002), and the ventilation rates were obtained by solving energy balances assuming a homogeneous air temperature

Submitted for review in June 2011 as manuscript number SE 9222; approved for publication by the Structures & Environment Division of ASABE in August 2011.

The authors are **Alejandro López,** Lecturer, **Diego L. Valera, ASABE Member,** Professor, **Francisco D. Molina-Aiz,** Associate Professor, and **Araceli Peña,** Professor, Department of Rural Engineering, University of Almería, Almería, Spain. **Corresponding author:** Diego L. Valera, Department of Rural Engineering, University of Almería, Carretera de Sacramento s/n, 04120 Almería, Spain; phone: +34-9500-15546; fax: +34-9500-15491; e-mail: dvalera@ual.es.

  ISSN 2151-0032

(Wang and Boulard, 2000; Demrati et al., 2001). Nevertheless, these techniques only allow prediction of a general air exchange rate in the greenhouse. Airflow has also been estimated directly through the vents by measuring the difference in pressure in different greenhouses (Kittas et al., 1996; Boulard et al., 1998).

In fact, air velocity measurements have been taken at vents and inside the greenhouse using unidimensional (Boulard et al., 1997a), two-dimensional (Wang and Deltour, 1999), and three-dimensional (3D) sonic anemometers (Wang and Deltour, 1997; Boulard et al., 1998; Boulard et al., 2000; Tanny et al., 2006; Katsoulas et al., 2007; Teitel et al., 2008; Kittas et al., 2008; Molina-Aiz et al., 2009; López et al., 2010). Some of these studies (Boulard et al., 1996; Boulard et al., 1997a) have shown the feasibility of direct measurements of airflow through the greenhouse vents. Teitel et al. (2008) calculated the ventilation rate by multiplying the average air velocity near the inlet and outlet openings (measured with a 3D sonic anemometer in the middle of the opening) by the area of the windows, obtaining ventilation rates similar to those obtained with N_2O tracer gas analysis. Moreover, sonic anemometry allows analysis of the airflow turbulence, which enhances heat transfer due to the increase of convective transport by turbulence and also results in mixing of substances and dispersal of momentum (Mathieu and Scott, 2000). An important characteristic of turbulence is its ability to transport and mix fluids much more effectively than a comparable laminar flow (Pope, 2009). Anemometric measurements have also allowed us to compare the level of turbulence in the airflow inside the greenhouse with different surrounding obstacles.

With a view to evaluating the possible effect of different obstacles close to greenhouse side vents, sonic anemometry has been used to study natural ventilation and the airflow characteristics at the plane of the ventilation openings of two greenhouses in different situations. The main aim of the present work was to quantify the drop in air velocity at the side vents given different scenarios (obstacles) and to study the characteristics of airflow in each case.

Material and Methods

Experimental Setup

The experimental work took place in two multi-span greenhouses (fig. 1a) located at the agricultural research farm belonging to the University of Almería (36°51′ N, 2° 16′ W) on the southern coast of Spain. The greenhouses were divided into two similar sectors by a polyethylene sheet fixed to a stainless steel structure (sectors 1a, 1b, 2a, and 2b; fig. 1a), as this allows us to study the natural ventilation of the two halves separately. The dimensions of the vents of each sector are specified in table 1.

In order to prevent insects entering the greenhouses, insect-proof screens were placed on all the vents. Valera et al. (2006) developed the methodology for the geometric (table 2) and aerodynamic characterization of the screens. The configuration of each sector was different according to the type of obstacle affecting the side vents (fig. 1a). The southern sides of both greenhouses face multi-tunnel greenhouses (6.75 m maximum height, 4.6 m at the perimeter) at a distance of 3 m. The northern side of greenhouse 2 faces an Almería-type greenhouse (4.7 m maximum height, 3.4 m at the perimeter) at a distance of 3 m. The northern part of the eastern side of greenhouse 1 faces a small warehouse (10 × 9 m^2, 6.75 m maximum height, 4.6 m at the perimeter) located at the northeastern corner of the greenhouse, while the northern part of the western side is free of obstacles (approx. 50 m away from a small hillock).

Equipment and Instrumentation

Outside climatic conditions were recorded by a meteorological station at a height of 10 m (fig. 1a). The meteorological station included a BUTRON II measurement box (Hortimax S.L., Almería, Spain) with a Pt1000 temperature sensor and a capacitive humidity sensor, with a temperature measurement range of -25°C to 75°C and accuracy of ±0.01°C, and a humidity range of 0% to 100% and accuracy of ±3%. Outside wind speed was measured with a Meteostation II (Hortimax S.L.), incorporating a cup anemometer with a measurement range of 0 to 40 m s^{-1},

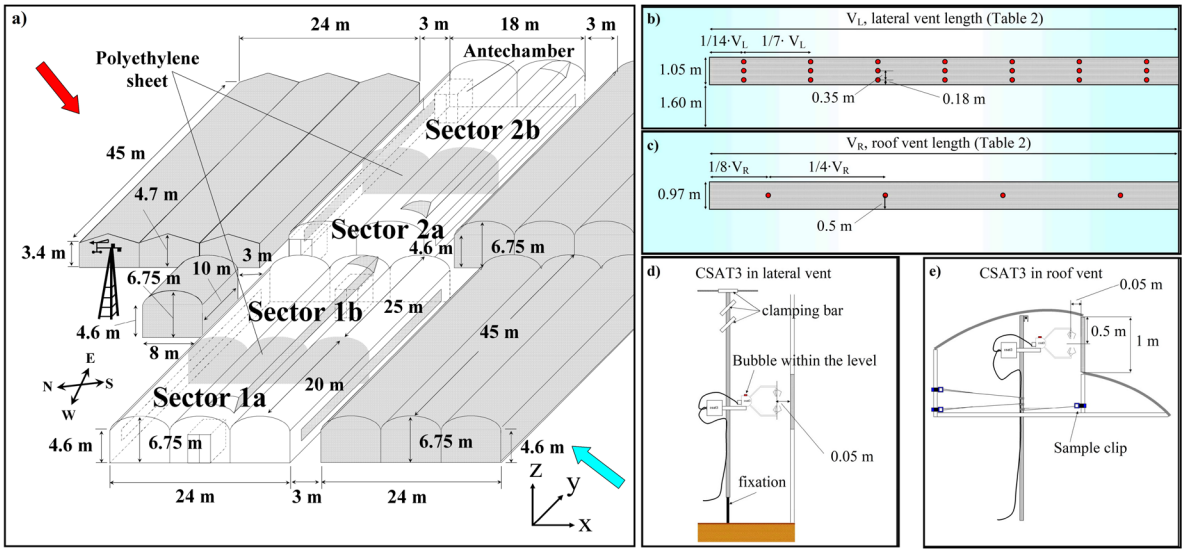

Figure 1. Location of the experimental greenhouses at the farm: (a) red arrow (upper left) indicates *Levante* wind and blue arrow (lower right) indicates *Poniente* wind; measurement points (red circles) at the (b) side vents and (c) roof vents; and positioning of the 3D sonic anemometer at the (d) side vents and (e) roof vents.

Table 1. Dimensions of the vents (m^2).

	Eastern Sectors (1b and 2b)			Western Sectors (1a and 2a)		
	Northern side vent	Southern side vent	Roof vent	Northern side vent	Southern side vent	Roof vent
Greenhouse 1	1.05 × 22.5	1.05 × 22.5	0.97 × 22.5	1.05 × 17.5	1.05 × 17.5	0.97 × 17.5
Greenhouse 2	1.05 × 20.0[a]	1.05 × 22.5	0.97 × 22.5	1.05 × 15.0[a]	1.05 × 17.5	0.97 × 17.5

[a] The length of these vents is lower due to the presence of two antechambers in the northern side of the greenhouse (fig. 1a).

Table 2. Geometric characteristics of the insect-proof screens placed in the different sectors of the greenhouse: D_f and D_r are the thread densities according to the manufacturer and measurement, respectively (threads cm^{-2}), φ is the porosity (%), L_{px} is the length of the pore in the direction of the warp (μm), L_{py} is the length of the pore in the direction of the weft (μm), D_h is the diameter of the threads (μm), D_i is the diameter of the inside circumference of the pore (μm), S_p is the average surface of the pore (mm^2), and e is the thickness (μm).

Sector	D_f	D_r	φ	L_{px}	L_{py}	D_h	D_i	S_p	e
1b and 2b	10 × 20	9.9 × 19.7	33.5	233.7	734.0	274.5	236.6	0.171	563.8
2a	14 × 27	12.9 × 26.8	38.5	188.4	591.6	184.4	191.3	0.111	401.7
1a	13 × 30	13.1 × 30.5	39.0	164.6	593.3	165.5	167.4	0.098	391.7

accuracy of ±5%, and resolution of 0.01 m s^{-1}. Wind direction was measured with a vane (accuracy ±5° and resolution 1°). Solar radiation was measured using a Kipp Solari (Hortimax S.L.) sensor, with a measurement range of 0 to 2000 W m^{-2}, accuracy of ±20 W m^{-2}, and resolution of 1 W m^{-2}.

Air velocity and sonic temperature (T_S) at the vents was measured with a 3D sonic anemometer (model CSAT3, Campbell Scientific Spain S.L., Barcelona, Spain; resolution: 0.001 m s^{-1} and 0.002°C; accuracy: ±0.04 m s^{-1} and ±0.026°C). Data were recorded by a CR3000 micro logger (Campbell Scientific Spain S.L.) with a data registration frequency of 10 Hz (Shilo et al., 2004; Molina-Aiz et al., 2009; López et al., 2010). For each measurement test, airflow was measured at 21 evenly distributed points at each side vent (fig. 1b). For this purpose, each side vent was divided into seven equal horizontal spaces and three vertical spaces. Air velocity measurements were taken at the center of each of the resulting 21 spaces. As it proved difficult to place the sonic anemometer at the roof vent, this vent was divided into four equal spaces along the main axis of the greenhouse, and the air velocity measurements were taken at the center of each space. Measurements were taken at each point over a 5 min period.

The wire frame intended to support and guide the crop was used to change the sonic anemometer position inside the greenhouse at the different measurement points. The anemometer was mounted to a horizontal arm, which was fixed to a 3 m long aluminum pipe (fig. 1d). At the upper end of the vertical pipe, three U-shaped clamps were attached in order to fix the pipe to the wire frame. These supports were attached 0.35 m apart in order to allow the height of the anemometer to be modified when placed in the side vents. At the lower end of the vertical pipe, a rod of smaller diameter was inserted to anchor the device to the ground once the anemometer had been placed at the correct level. A similar system was used to place the anemometer at the roof vent (fig. 1e). A steel cable was extended under the greenhouse roof parallel to the roof vent, from which the vertical aluminum pipe with the anemometer was suspended. Once the anemometer was placed at the correct level, the device was secured to the greenhouse structure.

The measurements were done under prevailing *Levante* (northeast) and *Poniente* (southwest) winds, the most usual winds in the province of Almería (Molina-Aiz et al., 2009). Measurements at the different positions were not done simultaneously, and therefore there may be an influence of the change in wind direction. The measurement tests were carried out around midday, when the cooling effect was most needed, and wind direction and solar radiation were more stable. Thus, the outside climatic conditions remained relatively stable over the measurement tests (table 3), with the exception of the test on April 2, 2008, in sector 2b (04/02/2008-2b), when there was a light *Poniente* wind of 0.7 to 2.74 m s^{-1} whose direction varied within the range 140° to 248°.

Due to the low density of measurement points at the roof vents in the present work, six additional assays were carried out to measure air speed only at these vents (recording data at five different heights at each measurement point). These results provided vertical profiles of air speed at the center of

Table 3. Outside climatic conditions: $\bar{u}_o$ is the mean wind speed during the measurement test (m s^{-1}), θ is the wind direction (°), RH_o is the relative outside humidity (%), T_o is the outside temperature (°C), R_g is the solar radiation (W m^{-2}), and ΔT_{io} is the difference of temperature between the inside and outside.

Wind	Date-Sector	Time	$\bar{u}_o$	θ[a]	RH_o	T_o	R_g	ΔT_{io}	$\bar{u}_o / \Delta T_{io}^{0.5}$
Levante	01/23/2008-1b	10:00-14:45	6.87 ±1.16	83 ±8	44 ±3	18.2 ±0.2	462 ±81	1.3	5.40
	03/29/2008-1a[b]	10:12-14:24	6.98 ±1.23	68 ±7	45 ±4	20.2 ±1.0	369 ±96	2.4	4.54
	04/05/2008-2a[b]	10:12-14:15	3.75 ±1.16	85 ±13	48 ±1	17.3 ±1.0	503 ±292	3.9	2.05
Poniente	01/30/2008-1a	10:05-14:55	3.39 ±0.61	264 ±14	71 ±4	14.8 ±0.5	504 ±41	5.6	1.13
	03/07/2008-2a	11:18-13:58	6.03 ±1.18	267 ±9	44 ±4	15.7 ±0.4	697 ±37	4.7	1.83
	03/15/2008-1b	11:06-14:13	4.43 ±1.76	257 ±13	81 ±4	17.4 ±0.7	467 ±176	5.4	1.50
	03/26/2008-1b[b]	10:18-14:25	6.14 ±1.60	256 ±9	65 ±4	17.2 ±0.9	760 ±70	7.5	1.74
	04/02/2008-2b[b]	10:22-14:37	1.72 ±1.02	194 ±54	34 ±7	18.6 ±1.4	552 ±290	5.5	0.79

[a] Direction perpendicular to the windows is 28° for *Levante* wind from northeast and 208° for *Poniente* wind from southwest.
[b] Air velocity measured only at the side vents.

each of the four areas into which the roof vent was divided. Thus, we can correct the mean values of u_x to calculate the airflow, multiplying u_x by a coefficient A_P obtained from the vertical profiles (A_P = 2.398 for *Levante* winds, and A_P = 0.718 for *Poniente* winds) (López, 2011).

The first two measurement tests (01/23/2008-1b and 01/30/2008-1a) were carried out in the presence of a tomato crop (*Solanum lycopersicum* L. cv. Pitenza) with an average height of 2 m and a leaf area index (LAI) of 1.3 m^2 m^{-2}. The lower leaves of the tomato plant were pruned to avoid the risk of disease. The presence of a crop can decrease the ventilation efficiency by as much as 28% (Boulard et al., 1997b). The other six tests were carried out in the empty greenhouses. The greenhouse, sector, and general conditions of each test are presented in table 3.

Temperature and humidity inside the greenhouse were measured using 24 autonomous data loggers (HOBO Pro Temp-HR U23-001, Onset Computer Corp., Bourne, Mass.). Six data loggers were placed in the center of each sector of the greenhouses. In greenhouse 1, they were placed in a vertical profile under the ridge of the three greenhouse spans at heights of 1 and 2 m. In greenhouse 2, they were placed in a vertical profile under the ridge of the two greenhouse spans and beneath the trough (lowest point of the roof) at heights of 1 and 2 m. These fixed devices measure a temperature range of -40°C to 70°C with an accuracy of ±0.18°C and relative humidity of 0% to 100% with an accuracy of ±2.5%. They were all programmed to register data at 0.5 Hz and were protected against direct solar radiation with a passive solar radiation open shield. From the inside humidity data, we can obtain the specific humidity (q) and correct the sonic anemometer temperature (T_{SC}) using the following expression (Tanny et al., 2008):

$$T_{SC} = \frac{T_S}{1 + 0.51q} \tag{1}$$

Analyses

For air velocity (u) and its components (longitudinal u_x, transversal u_y and vertical u_z; fig. 1), the mean air velocity measured over a period Δt is (Cebeci, 2004):

$$\bar{u} = \frac{1}{\Delta t}\int_{t}^{t+\Delta t} u\,dt \tag{2}$$

The time interval Δt must be longer than any significant fluctuation and short enough for the transitory real-time effects not to affect the integration, and so its value was fixed at 5 min. The total duration of the assays varied between approximately 3 and 4 h (table 3). This time period is a compromise between a shorter period that may reduce accuracy and a longer period that may increase the overall difference with regard to outside microclimate parameters (Molina-Aiz et al., 2009). At each point, the sonic anemometer measured at a sampling rate of 10 Hz for 5 min. Calculations were made for each of the 1 min periods (600 data) and for the whole 5 min period (3000 data), ensuring that the data were coherent over time. In equation 3, $u(t)$ is the instantaneous air velocity, which can be expressed as the sum of time-mean value of u and a fluctuating component $u'(t)$ (Cebeci, 2004):

$$u(t) = \bar{u} + u'(t) \tag{3}$$

An instantaneous velocity is the average velocity plus the difference of the reading from the mean value. Turbulence is the variance of u'. The variance of an air velocity over a period of time Δt is defined as (Heber et al., 1996):

$$\sigma^2 = \overline{u'^2} = \frac{1}{\Delta t}\int_{t}^{t+\Delta t} (u - \bar{u})^2 dt \tag{4}$$

Turbulence intensity (i) is standard deviation σ divided by mean local velocity u (Cebeci, 2004):

$$i = \frac{\sqrt{\overline{u'^2}}}{\bar{u}} = \frac{\sigma}{\bar{u}} \tag{5}$$

Total turbulence kinetic energy (k, m^2 s^{-2}) can be calculated by the following expression (Loomans, 1998):

$$k = \frac{1}{2}\left(\sigma_x^2 + \sigma_y^2 + \sigma_z^2\right) \tag{6}$$

where σ_x, σ_y, and σ_z are the standard deviations of the three air velocity components.

Results and Discussion

Airflow Direction

At the side opening, the airflow was mainly horizontal, while at the roof vent it was upward or downward. In areas where there was an obstacle at the side vent, for example close to the warehouse located at the northeastern corner of greenhouse 1, or at the southern side vents of both greenhouses, the air velocity recorded was less and there were more fluctuations in the airflow (fig. 2 and table 4). In the case presented in figure 2, the Almería-type greenhouse that obstructs the northern side vent of greenhouse 2 is lower than the multi-span greenhouse obstructing the southern side vent. Consequently, the northern vent is more exposed to the wind.

In conditions of *Levante* wind, the ratio $u_o/\Delta T_{io}^{0.5}$ was always well above 1 (table 3), which would indicate that the chimney effect does not play a determining role in the greenhouse ventilation (Kittas et al., 1997). Given the location of the vents, the air must exit the greenhouse through the roof vent on the leeward side. Thus, the wind effect and

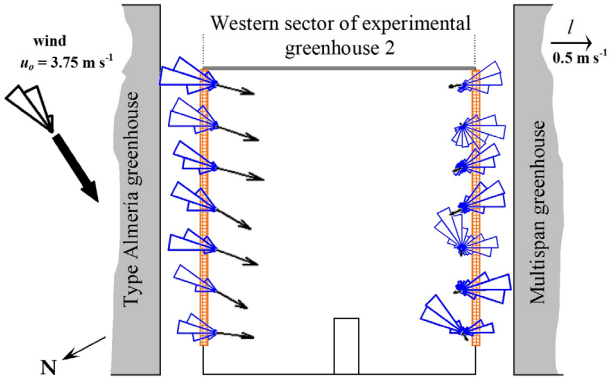

Figure 2. Two-dimensional resultants of air velocity on the *XY* plane (*l*) and polar plots of airflow direction for measurement test on 04/05/2008-2a (middle of the side vent).

Table 4. Average values (m s^{-1}) of air velocity (u, mean ±σ), intensity of turbulence (i), and turbulence kinetic energy (k, m^2 s^{-2}) at the vents. Subscripts x indicates longitudinal (normal) component, y indicates transversal component, and z indicates vertical component. Superscript n means normalized.

Date-Sector	Vent[a]	u_x[b]	$u_x{}^n$ [b]	u_y	u_z	i_x	i_y	i_z	i_u	k
Levante wind										
01/23/2008-1b	N	0.27 ±0.32	0.052	-0.14 ±0.10	-0.10 ±0.07	1.03 ±0.53	0.81 ±0.27	0.62 ±0.40	0.86 ±0.32	0.11
	S	0.15 ±0.20	0.020	-0.06 ±0.09	0.04 ±0.04	1.14 ±0.66	0.74 ±0.30	0.51 ±0.27	0.83 0.32	0.04
	R	-0.18 ±0.03	-0.027	0.15 ±0.13	0.47 ±0.10	0.29 ±0.09	0.32 ±0.09	0.38 ±0.13	0.31 ±0.06	0.05
03/29/2008-1a	N	0.95 ±0.22	0.147	-0.80 ±0.26	-0.21 ±0.13	0.40 ±0.08	0.53 ±0.09	0.18 ±0.04	0.53 ±0.09	0.42
	S	0.28 ±0.10	0.040	-0.01 ±0.05	0.07 ±0.06	1.21 ±0.49	0.62 ±0.27	0.52 ±0.17	0.87 ±0.28	0.08
04/05/2008-2a	N	0.42 ±0.23	0.115	-0.15 ±0.09	-0.14 ±0.12	0.65 ±0.54	0.44 ±0.26	0.32 ±0.32	0.62 0.40	0.06
	S	0.07 ±0.08	0.024	-0.03 ±0.04	0.08 ±0.09	0.85 ±0.36	0.67 ±0.28	0.69 ±0.26	0.66 ±0.25	0.03
Poniente wind										
01/30/2008-1a	N	-0.15 ±0.03	-0.088	-0.05 ±0.04	-0.01 ±0.02	0.46 ±0.11	0.25 ±0.08	0.28 ±0.08	0.36 ±0.07	0.01
	S	-0.08 ±0.06	-0.039	-0.06 ±0.06	0.03 ±0.04	0.71 ±0.44	0.51 ±0.31	0.57 ±0.30	0.50 0.22	0.01
	R	0.35 ±0.01	0.219	0.13 ±0.12	-0.11 ±0.03	0.48 ±0.07	0.55 ±0.03	0.50 ±0.07	0.59 ±0.02	0.08
03/07/2008-2a	N	-0.47 ±0.04	-0.104	-0.31 ±0.11	0.10 ±0.07	0.32 ±0.08	0.23 ±0.07	0.23 ±0.09	0.27 ±0.06	0.04
	S	-0.08 ±0.12	-0.027	-0.10 ±0.07	0.01 ±0.04	1.50 ±0.88	1.20 ±0.83	1.36 ±1.01	1.08 ±0.68	0.04
	R	0.58 ±0.22	0.180	0.28 ±0.04	-0.12 ±0.22	0.54 ±0.11	0.55 ±0.11	0.59 ±0.22	0.55 ±0.06	0.25
03/15/2008-1b	N	-0.10 ±0.22	-0.052	0.00 ±0.06	0.13 ±0.21	0.76 ±0.57	0.51 ±0.31	0.68 ±0.49	0.53 ±0.29	0.03
	S	-0.06 ±0.03	-0.018	-0.04 ±0.07	0.19 ±0.05	0.59 ±0.10	0.54 ±0.10	0.52 ±0.11	0.47 ±0.10	0.02
	R	0.52 ±0.10	0.157	0.20 ±0.10	-0.14 ±0.06	0.57 ±0.14	0.78 ±0.16	0.58 ±0.11	0.69 ±0.11	0.27
03/26/2008-1b	N	-0.18 ±0.12	-0.046	-0.04 ±0.12	0.24 ±0.11	0.49 ±0.17	0.47 ±0.17	0.51 ±0.22	0.41 ±0.12	0.04
	S	-0.10 ±0.09	-0.018	-0.06 ±0.12	0.22 0.06	0.76 ±0.17	0.69 ±0.24	0.69 ±0.29	0.55 ±0.16	0.05
04/02/2008-2b	N	0.04 ±0.08	0.045	0.02 ±0.03	-0.06 ±0.07	0.61 ±0.30	0.40 ±0.24	0.59 ±0.34	0.48 ±0.23	0.01
	S	0.06 ±0.07	0.044	0.04 ±0.06	0.05 ±0.11	0.83 ±0.34	0.73 ±0.29	0.83 ±0.42	0.70 ±0.26	0.03

[a] N = northern side vent, S = southern side vent, and R = roof vent.
[b] u_x and $u_x{}^n$ are positive for an inflow and negative for an outflow.

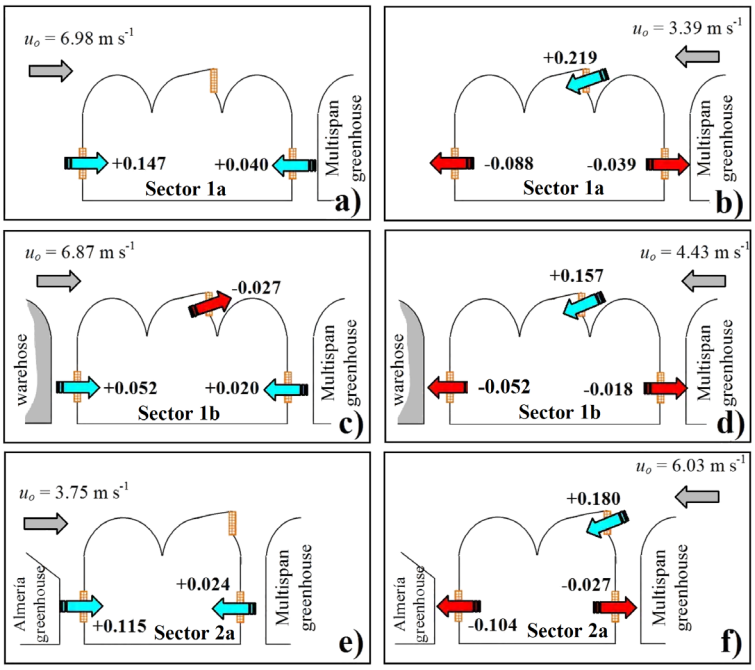

Figure 3. Average values of normalized longitudinal air velocity ($u_x{}^n$) at the vents for the different measurement tests. Assays with *Levante* wind (a) in sector 1a on 03/29/2008, (c) in sector 1b on 01/23/2008, and (e) in sector 2a on 04/05/2008. Assays with *Poniente* wind (b) in sector 1a on 01/30/2008, (d) in sector 1b on 03/15/2008, and (f) in sector 2a on 03/07/2008.

the chimney effect complement one another. The air enters through the northern side vent due to the wind effect and rises due to the pressure difference caused by wind and due to buoyancy before leaving through the roof vent, helped by the suction of the wind at this vent (figs. 3a, 3d, and 3g).

In situations of *Poniente* wind, on the other hand, the roof vent is windward and the windward side vent is completely blocked, and so the air tends to enter the greenhouse through the roof vent due to the wind effect and to exit through the northern, leeward side vent. In this case, the chimney effect,

which causes warm air to rise due to buoyancy, counteracts the wind effect, and the flow can be either upward or downward depending on the relative strengths of the two forces (Li and Delsante, 2001). Thus, in the tests in which the ratio $u_o/\Delta T_{io}^{0.5}$ was higher than 1, the air tended to enter through the roof vent and exit through both side vents (figs. 3b, 3e, and 3h). On the single occasion with a weak *Poniente* wind on 04/02/2008-2b, the ratio $u_o/\Delta T_{io}^{0.5}$ was less than 1 ($u_o/\Delta T_{io}^{0.5} = 0.79$) and the mean air velocity at the side vents was very low (0.04 ±0.08 m s^{-1} at the northern side vent and 0.06 ±0.07 m s^{-1} at the southern one; air velocity was not recorded at the roof vent), giving rise to similar amounts of air entering and exiting through the side vents. Thus, in the test on 04/02/2008-2b, although conditions were less stable, due to the wind effect, air entered through the roof vent and left through the side ones. However, the chimney effect caused warm air to rise, making the cool outside air enter through the side vents.

Normalized Longitudinal Air Velocity Component

The normalized velocity is of particular interest in order to calculate the average velocities at the plane of the ventilation openings and to compare the measurement tests carried out under different wind conditions. The normalized velocity at each measurement point j can be calculated as (Boulard et al., 2000):

$$u_j^n(t) = \frac{u_j(t)}{u_o(t)} \quad (7)$$

where $u_j(t)$ is the air velocity measured for the time interval corresponding to point j, and $u_o(t)$ is the average wind speed over the same time interval.

The presence of obstacles at the side vents gives rise to considerable drops in normalized air velocity. Comparison of normalized air velocity allow us analyze the effect on ventilation (independently of wind speed) of the different obstacles placed next to the side vents of the four sectors where air velocity was measured. The maximum value of u_x^n was recorded at the northern side vent (windward vent) in the measurement test on 03/29/2008-1a (fig. 3a) with *Levante* wind ($u_x^n = 0.147 \pm 0.072$). Regarding the obstacles located on the northern side of the two greenhouses (fig. 1a), when the northern vent is on the windward side for *Levante* wind, there is a 65% reduction in u_x^n caused by the warehouse at the northeastern corner of greenhouse 1 (fig. 3c), and a 22% reduction due to the Almería-type greenhouse (fig. 3e). Both these reductions are in comparison to the mean value observed in the western sector of greenhouse 1, which was free of obstacles (fig. 3a).

When the northern vent is on the leeward side (for *Poniente* wind), the influence of the obstacle does not appear to be so direct or clear, possibly due to the important role of the chimney effect under such conditions, since the maximum values of u_x^n were observed in greenhouse 2, which borders on the Almería-type greenhouse (fig. 3f), and in the western sector of greenhouse 1, which is free of obstacles (fig. 3b). However, we can observe a reduction of 28% in the normalized velocity ($u_x^n = 0.157$) at the roof vent when the warehouse blocks the exit of air through the leeward side vent (fig. 3d), in comparison to the mean value ($u_x^n = 0.219$) observed in the western sector of greenhouse 1, which is free of obstacles (fig. 3b). This reduction is only of 18% ($u_x^n = 0.180$) when the northern side vent is obstructed by an Almería-type greenhouse (fig. 3f). The rise in the height of the obstacle placed next to the side vent (4.7 m for the Almería-type greenhouse and 6.75 m for the warehouse) produces an increase in the blocking effect over the greenhouse ventilation.

The normalized velocity of the longitudinal component (u_x^n, perpendicular to the vents) was greater at the northern side vent, which is more exposed to the wind than the southern one, for both *Levante* and *Poniente* winds (fig. 3 and table 4). The reduction in u_x^n at the southern side vent, which faces another multi-span greenhouse, when compared to the northern side vent, has been calculated as 61%, 73%, and 79% for the measurement tests with *Levante* wind on 01/23/2008-1b, 03/29/2008-1a, and 04/05/2008-2a, respectively, and as 56% and 60% for the measurement tests carried out with *Poniente* wind on 01/30/2008-1a and 03/26/2008-1b, respectively. In conditions of *Poniente* wind, the ratio $u_o/\Delta T_{io}^{0.5}$ was less than 1 (04/02/2008-2b), and no differences were observed between the air velocities at the side vents (table 4, fig. 3f). Whenever the chimney effect prevails in conditions of weak wind, the ventilation rate is much less affected by the presence of obstacles outside the greenhouse.

The obstacles partially blocking the northern side vent in the eastern sector of greenhouse 1 mean that the differences observed between the mean values of normalized air velocity at the side vents may be misleading. The warehouse obstructs the first 7.5 m of the northern side vent of the eastern sector of greenhouse 1 (fig. 1a), affecting mainly the six measurement points nearest the eastern end of the vent. If we calculate the mean air velocity in the zone of the northern vent that has no obstacles, then the difference with the southern side vent is greater. For instance, in the test on 01/23/2008-1b, the mean value of u_x^n in the part of the northern vent that is blocked by the warehouse was 0.000 ±0.002. The obstacle hindered the airflow in that part of the vent, whereas in the part that is free of obstacles u_x^n was 0.073 ±0.027, three (3.64) times greater than at the southern side vent. In the test on 03/26/2008-1b, the situation was similar, as the mean value of u_x^n in the part of the northern vent with the obstacle was -0.028 ±0.007, as opposed to -0.053 ±0.031 in the part without obstacles, i.e., three (2.94) times greater than at the southern vent. In the test on 03/15/2008-1b, the situation was somewhat different, since in the part of the northern vent with obstacle there was inflow of air (u_x^n = 0.004 ±0.039), while in the part without obstacles there was outflow (u_x^n = -0.021 ±0.010), slightly higher than at the southern side vent. Molina-Aiz et al. (2009) also observed that an obstacle close to the side vent in an Almería-type greenhouse can produce simultaneous inflow and outflow in different parts of the opening.

Katsoulas et al. (2006) also observed the influence of obstacles on a single-tunnel greenhouse with insect-proof screens, recording a 67% reduction in u_x^n in comparison with the vent that had no obstruction. Kittas et al. (2008) also observed reduced normalized velocity at one of the side vents due to the proximity of another greenhouse (4.5 m away), recording mean u_x^n values at the unobstructed vent of 0.070 ±0.015 with screen and 0.392 ±0.050 without screen, compared to 0.039 ±0.022 with screen and 0.138 ±0.050 without screen at the vent with obstacles. This constitutes a

reduction in velocity of 44% with screen and 65% without screen.

The normalized velocity recorded at the different ventilation surfaces on occasion was higher than the maxima recorded by Molina-Aiz et al. (2009) in an Almería-type greenhouse with insect-proof screens ($u_x{}^n$ = 0.053 at the windward side vent with *Poniente* wind of 3.89 m s^{-1} and $u_x{}^n$ = 0.063 at the roof vent with *Levante* wind of 8.4 m s^{-1}). It was similar to the values observed by Teitel et al. (2008) at the windward side vent of a single-span greenhouse with two side vents and no roof vent ($u_x{}^n$ = 0.11 ±0.05).

Estimation of Air Exchange Rates

The mean volumetric airflow (G_M) has been calculated as the average of the sum of the inflows (positive values of G) at the different vents and of the sum of the outflows (negative values of G). With only one sampling position possible at any one time, a difficulty arises concerning how to deal with changing external conditions over the time needed to measure airflow at the 46 different positions (fig. 1b). This problem can be overcome by selecting measurements for a fixed external wind direction and correcting the air velocities measured by the 3D sonic anemometer at each position j at the greenhouse openings $u_j(t)$ through a process of scaling with the wind speed (Molina-Aiz et al., 2009). Multiplying measured values of air velocity $u_j(t)$ at minute t at each point j in the greenhouse openings by the ratio between the average wind speed u_o for the overall test period (several hours) and the instantaneous values $u_o(t)$ (average for each minute t) (Molina-Aiz et al., 2009), as follows:

$$u_j^*(t) = u_j(t)\frac{\overline{u}_o}{u_o(t)} \quad (8)$$

In addition to correcting the longitudinal component with the wind speed, we applied the correction coefficients obtained from the vertical profile of speeds at the roof vent (López, 2011).

The error in calculation of the average air exchange rate was estimated by the method of conservation of the mass of air as the sum of the flow at each of the vents (table 5). The sum of the airflows entering the greenhouse must be equal to the sum of the flows leaving it, assuming a certain degree of error due to the fact that the measurements were not simultaneous at the different points in the vents, and to the change in climatic conditions during the tests and/or to the insufficient density of measurement points. In the measurement tests on 01/23/2008-1b, 01/30/2008-1a, 03/07/2008-2a, and 03/15/2008-1b, measuring the airflow at the two side vents and the roof vent, the error of flows recorded was 1.0%, 21.9%, 27.6%, and 12.3%, respectively. The errors calculated are close to those obtained by other authors. In an Almería-type greenhouse with two side and two roof vents, Molina-Aiz et al. (2009) obtained errors in the range of 3% to 37%. In a multi-span greenhouse with a single roof vent, Boulard et al. (1996) obtained errors of 2.2% to 2.6% measuring the airflow with a one-dimensional sonic anemometer. In the same circumstances, using a three-dimensional sonic anemometer, they obtained an error of 31.6% (Boulard et al., 1997a). When measurements were only taken at the side vents, the air exchange rate was estimated taking into account that the airflow at the side vents must be equal to the airflow at the roof vent.

The observed maximum values of air exchanges (31.6 h^{-1} for *Levante* wind and 12.7 h^{-1} for *Poniente* wind) are below the 35 to 90 h^{-1} recommended for greenhouses (*ASABE Standards*, 2003) and the optimum value of 45 to 60 h^{-1} (Hellickson and Walker, 1983; *ASABE Standards*, 1994). In general, they approach the values observed with natural ventilation in the province of Almería (5 to 15 h^{-1}) in Almería-type greenhouses (Molina-Aiz et al., 2009) and in multi-span greenhouses (Valera et al., 2009).

For *Levante* winds, the greatest number of air renewals was recorded in the western sector of greenhouse 1 (free of obstacles), with the highest wind speed and with the wind direction more perpendicular to the side vent. In the first assay carried out with crop and with *Levante* wind (01/23/2008-1b), the air exchange rate was less than in the test on 04/05/2008-2a (fig. 4) carried out without a crop, although the wind speed was higher. This may be due to the reduction of ventilation caused by the crop, as observed by Boulard et al. (1997b).

For *Poniente* winds, although the only assay in the western sector of greenhouse 1, which is free from obstacles, was carried out (with a crop) on a day with low wind speed (01/30/2008-1a), a higher number of air exchanges was obtained than in other assays when the wind speed was greater, in other sectors with greater obstacles (fig. 4 and table 5).

A slight increase was observed in the air exchange rate with prevailing *Levante* wind (fig. 4), since the windward side vent was more exposed in these circumstances (fig. 1a). As the roof vent was on the leeward side, the wind effect and chimney effect complement one another, making the natural

Table 5. Corrected longitudinal component (u_x, m s^{-1}), airflow at each vent (G, m^3 s^{-1}), mean airflow (G_M, m^3 s^{-1}), ventilation rate (R_M, air exchanges per hour), and error in the calculation of airflows (%).

		u_x[a]			G					
	Date-Sector	N[b]	S	R[c]	N	S	R	G_M	R_M	Error
Levante wind	01/23/2008-1b	0.284	0.126	-0.449	6.7	3.0	-9.8	9.7	10.3	1.0%
	03/29/2008-1a	1.027	0.279	--	18.9	5.1	--	24.0	31.6	--
	04/05/2008-2a	0.468	0.099	--	7.4	1.8	--	9.2	15.4	--
Poniente wind	01/30/2008-1a	-0.204	-0.103	0.421	-3.8	-1.9	7.1	6.4	8.4	21.9%
	03/07/2008-2a	-0.406	-0.092	0.512	-5.2	-1.4	8.7	7.6	12.7	27.6%
	03/15/2008-1b	-0.233	-0.057	0.354	-5.5	-1.3	7.7	7.3	7.7	12.3%
	03/26/2008-1b	-0.219	-0.086	--	-5.2	-2.0	--	7.2	7.6	--
	04/02/2008-2b	0.082	0.081	--	1.7	1.9	--	3.6	4.9	--

[a] Positive for an inflow and negative for an outflow.
[b] N = northern side vent; S= southern side vent; and R = roof vent.
[c] At the roof vent, coefficient A_P is applied bearing in mind the vertical profile of speeds obtained in the other tests.

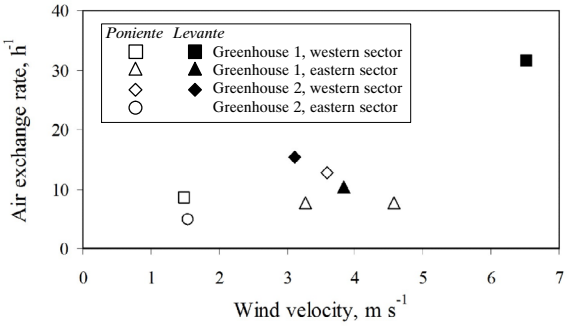

Figure 4. Measured air exchange rate against wind speed (perpendicular to the side vents) for tests under prevailing *Poniente* and *Levante* winds.

ventilation more effective. In order to make an objective evaluation of the effect of ventilation on the temperature of the inside air, we have used the term "ventilation efficiency for temperature" (η_T). The efficiency of a ventilation system can be related to the temperature inside the greenhouse and that of the air leaving through the vents as follows (Qingyan et al., 1988; Tanny et al., 2008; Molina-Aiz et al., 2011):

$$\eta_T = \frac{T_{ov} - T_o}{\Delta T_{io}} \quad (9)$$

where T_{ov} is the average temperature of the air exiting the vents, calculated as the mean of sonic temperatures T_{SC} (eq. 1) at all the points where air leaves the greenhouse, and ΔT_{io} is the difference between the inside and outside temperatures during the measurement test. The inside temperature is calculate by the average of the six measurements obtained from the data loggers placed inside the greenhouses. The term η_T represents the effectiveness in eliminating the heat from the area of the greenhouse occupied by the crop. When the air inside the greenhouse mixes perfectly, $\eta_T = 1$ (Tanny et al., 2008; Molina-Aiz et al., 2011). Generally speaking, ventilation has been found to be more efficient for temperature with *Levante* winds (mean value for the three tests of $\eta_T = 1.61$) than with *Poniente* winds (mean value for the five tests of $\eta_T = 0.59$). With prevailing *Levante* winds, the vent with fewest obstacles is on the windward side, which favors the flow of air in through the side vents and out through the roof vent. This may have led to a greater temperature gradient (ΔT_{io}) in the assays with *Poniente* wind than in those with *Levante* (table 3).

Turbulence Flow Characteristics

The mean levels of turbulence intensity (table 4) recorded at the plane of the ventilation openings were similar to those described by Tanny et al. (2006) for the interior of a greenhouse that is of similar structure to the Almería-type but with a net covering ($\varphi = 0.83$), known as a "banana screenhouse". In this case, the turbulence intensity (i) varied between 0.2 and 0.8 for wind speeds <0.5 m s^{-1} and it stayed at around 0.5 for higher wind speeds.

The presence of obstacles close to the sides of the greenhouse causes increases in the intensity of airflow turbulence close to the side vents (table 4). The mean value of turbulence intensity for the component of air velocity perpendicular to the windows (i_x) was greater at the southern side vent, with more obstacles, than at the northern side vent.

Tanny et al. (2008) studied the airflow in an experimental device consisting of a box with ventilation openings on the upper and lower sides, finding the maximum levels of turbulence intensity in the area where the inflow and outflow of air mixed, due to higher shear stress and higher velocity gradients. Teitel et al. (2008) determined the turbulence intensity at the plane of the ventilation openings of a single-tunnel greenhouse with side vents, finding that it was higher at the windward vent ($i_x = 0.35$) than at the leeward vent ($i_x = 0.21$). Both vents were free of obstacles.

In our opinion, the fact that with *Levante* winds the turbulence intensity at the leeward vent is greater than at the windward vent, unlike the findings of Teitel et al. (2008), may be due to the greater presence of obstacles on the southern side of the two greenhouses used in the tests.

In conditions of prevailing *Poniente* winds, greater turbulence intensity was also recorded at the southern vent with more obstacles. One exception was recorded in greenhouse 1 in the test on 03/15/2008-1b, when there was an increase in turbulence intensity in the part of the northern side vent closest to the neighboring warehouse, meaning that the mean values calculated for the northern and southern side vents were similar. In the part of the northern vent closest to the warehouse, i_x was 1.17 ±0.55, compared to 0.34 ±0.08 in the part without obstacles. The mean value of i_x at the southern vent was 0.59 ±0.10, i.e., higher than the value recorded at the part of the northern vent without obstacles.

An increase in turbulence intensity due to outside obstacles was also noted by Molina-Aiz et al. (2009) in an Almería-type greenhouse. In this case, the obstacle was an advertising hoarding 1.6 m from one of the side vents. For these authors, the turbulence intensity was greater at the vent with obstacles both when it was on the windward side (i_x = 0.94) and when it was leeward ($i_x = 2.74$). Indeed, the values recorded at the other vent were considerably lower ($i_x = 0.34$ and $i_x = 0.65$, respectively).

An important characteristic of turbulence is its ability to transport and mix fluids much more effectively than a comparable laminar flow (Pope, 2009). In the present case, as the southern side vent had obstacles, although the turbulence intensity increased, there was a reduction in air velocity and turbulence kinetic energy k (table 4). Consequently, there was also a reduction in the ability of the air to mix and transport heat and water vapor.

Under conditions of prevailing *Levante* winds, the airflow was much more energetic at the northern, windward side vent that was free of obstacles than at the southern side vent. Similar results were obtained by Boulard et al. (2000). However, at the southern side vent, as the same type of obstacle was present in all cases, there was not such a great difference in the level of energy depending on the prevailing wind (table 4).

Conclusions

A gap of 3 m between greenhouses has been shown to be insufficient to avoid the influence of the obstacles on the natural ventilation of the greenhouse. The minimum distance to maintain between greenhouses, or between a greenhouse and any other building, will depend on the geometry of the obstacle (mainly its height).

An increase in the height of an obstacle placed next to the side vent (from 4.7 to 6.75 m) produces an increase in the blocking effect over the greenhouse ventilation. When the blocked vent was on the windward side of the greenhouse (working as an air entrance), reduction in the normalized velocity (measured in this vent) increased from 22% to 65%, in comparison with a side vent free of obstacles. When the blocked vent was on the leeward side of the greenhouse (working as an air exit), reduction in the normalized velocity measured in the roof vent, through which air enters the greenhouse, increased from 18% to 28%.

In the case studied, i.e., greenhouses with two side vents, one of which has obstructions, and one roof vent, natural ventilation was more efficient for the temperature ($\eta_T > 1$) when the vent with fewer obstructions was on the windward side and the roof vent was on the leeward side, favoring the flow of air in through the side vents and out through the roof vent.

The presence of obstacles at the side vents has also been shown to reduce the turbulent kinetic energy of the airflow, and therefore its capacity to mix air and transport heat.

ACKNOWLEDGEMENTS

This work was founded by projects AGL2010-22284-C03-01 of Ministerio de Ciencia e Innovación of Spain and P09-AGR-4593 of Junta de Andalucía.

REFERENCES

ASABE Standards. 1994. EP406.1: Heating, ventilating, and cooling greenhouses. St. Joseph, Mich.: ASAE.

ASABE Standards. 2003. EP406.4 JAN03 (R2008): Heating, ventilating, and cooling greenhouses. St. Joseph, Mich.: ASAE.

Baptista, F. J., B. J. Bailey, J. M. Randall, and J. F. Meneses. 1999. Greenhouse ventilation rate: Theory and measurement with tracer gas techniques. *J. Agric. Eng. Res.* 72(4): 363-374.

Bot, G. P. A. 1983. Greenhouse climate: From physical processes to a dynamic model. PhD diss. Wageningen, The Netherlands: Agricultural University of Wageningen.

Boulard, T., and A. Baille. 1995. Modelling of air exchange rate in a greenhouse equipped with continuous roof vents. *J. Agric. Eng. Res.* 61(1): 37-48.

Boulard, T., and B. Draoui. 1995. Natural ventilation of a greenhouse with continuous roof vents: Measurements and data analysis. *J. Agric. Eng. Res.* 61(1): 27-36.

Boulard, T., J. F. Meneses, M. Mermier, and G. Papadakis. 1996. The mechanisms involved in the natural ventilation of greenhouses. *Agric. Forest Meteorol.* 79(1): 61-77.

Boulard, T., G. Papadakis, C. Kittas, and M. Mermier. 1997a. Airflow and associated sensible heat exchanges in a naturally ventilated greenhouse. *Agric. Forest Meteorol.* 88(1-4): 111-119.

Boulard, T., P. Feuilloley, and C. Kittas. 1997b. Natural ventilation performance of six greenhouse and tunnel types. *J. Agric. Eng. Res.* 67(4): 249-266.

Boulard, T., C. Kittas, G. Papadakis, and M. Mermier. 1998. Pressure field and airflow at the opening of a naturally ventilated greenhouse. *J. Agric. Eng. Res.* 71(1): 93-102.

Boulard, T., S. Wang, and R. Haxaire. 2000. Mean and turbulent airflows and microclimatic patterns in an empty greenhouse tunnel. *Agric. Forest Meteorol.* 100(2-3): 169-181.

Bruce, J. M. 1978. Natural convection through openings and its applications to cattle building ventilation. *J. Agric. Eng. Res.* 23(2): 151-167.

Bruce, J. M. 1982. Ventilation of a model livestock building by thermal buoyancy. *Trans. ASAE* 25(6): 1724-1726.

Cebeci, T. 2004. *Analysis of Turbulent Flows*. Amsterdam, The Netherlands: Elsevier.

Demrati, H., T. Boulard, A. Bekkaoui, and L. Bouirden. 2001. Natural ventilation and microclimatic performance of a large-scale banana greenhouse. *J. Agric. Eng. Res.* 80(3): 261-271.

Fernandez, J. E., and B. J. Bailey. 1992. Measurement and prediction of greenhouse ventilation rates. *Agric. Forest Meteorol.* 58(3-4): 229-245.

Heber, A. J., C. R. Boon, and M. W. Peugh. 1996. Air patterns and turbulence in an experimental livestock building. *J. Agric. Eng. Res.* 64(3): 209-226.

Hellickson, M. A., and J. N. Walker. 1983. *Ventilation of Agricultural Structures.* ASAE Monograph No. 6. St. Joseph, Mich.: ASABE.

Katsoulas, N., T. Bartzanas, T. Boulard, M. Mermier, and C. Kittas. 2006. Effect of vent openings and insect screens on greenhouse ventilation. *Biosyst. Eng.* 93(4): 427-436.

Katsoulas, N., A. Baille, and C. Kittas. 2007. Leaf boundary layer conductance in ventilated greenhouses: An experimental approach. *Agric. Forest Meteorol.* 144(3-4): 180-192.

Kittas, C., B. Draoui, and T. Boulard. 1995. Quantification of the ventilation rate of a greenhouse with a continuous roof opening. *Agric. Forest Meteorol.* 77(1): 95-111.

Kittas, C., T. Boulard, M. Mermier, and G. Papadakis. 1996. Wind-induced air exchange rates in a greenhouse tunnel with continuous side openings. *J. Agric. Eng. Res.* 65(1): 37-49.

Kittas, C., T. Boulard, and G. Papadakis. 1997. Natural ventilation of a greenhouse with ridge and side openings: Sensitivity to temperature and wind effects. *Trans. ASAE* 40(2): 415-425.

Kittas, C., T. Boulard, T. Bartzanas, N. Katsoulas, and M. Mermier. 2002. Influence of an insect screen on greenhouse ventilation. *Trans. ASAE* 45(4): 1083-1090.

Kittas, C., N. Katsoulas, T. Bartzanas, M. Mermier, and T. Boulard. 2008. The impact of insect screens and ventilation openings on the greenhouse microclimate. *Trans. ASABE* 51(6): 2151-2165.

Li, Y., and A. Delsante. 2001. Natural ventilation induced by combined wind and thermal forces. *Build. Environ.* 36(1): 59-71.

Loomans, M. G. L. C. 1998. The measurement and simulation of indoor airflow. MS thesis. Eindhoven, The Netherlands: Technische Universiteit Eindhoven.

López, A. 2011. Contribución al conocimiento del microclima de los invernaderos mediterráneos mediante anemometría sónica y termografía. PhD diss. Almería, Spain: University of Almería, Department of Rural Engineering.

López, A., D. L. Valera, F. D. Molina-Aiz, and A. A. Peña. 2010. Experimental evaluation by sonic anemometry of airflow in a Mediterranean greenhouse equipped with a pad-fan cooling system. *Trans. ASABE.* 53(3): 945-957.

Mathieu, J., and J. Scott. 2000. *An Introduction to Turbulent Flow.* Cambridge, U.K.: Cambridge University Press.

Molina-Aiz, F. D., D. L. Valera, A. A. Peña, J. A. Gil, and A. López. 2009. A study of natural ventilation in an Almería-type greenhouse with insect screens by means of tri-sonic anemometry. *Biosyst. Eng.* 104(2): 224-242.

Molina-Aiz, F. D., D. L. Valera, A. López, and A. J. Álvarez. 2011. Analysis of cooling ventilation efficiency in a naturally ventilated Almería-type greenhouse with insect screens. *Acta Hort.* (in press).

Montero, J. I., A. Anton, R. Kamaruddin, and B. J. Bailey. 2001. Analysis of thermally driven ventilation in tunnel greenhouses using small scale models. *Biosyst. Eng.* 79(2): 213-222.

Papadakis, G., M. Mermier, J. F. Meneses, and T. Boulard. 1996. Measurement and analysis of air exchange rates in a greenhouse with continuous roof and side openings. *J. Agric. Eng. Res.* 63(3): 219-228.

Pérez-Parral, J., E. Baeza, J. I. Montero, and B. J. Bailey. 2004. Natural ventilation of parral greenhouses. *Biosyst. Eng.* 87(3): 355-366.

Pope, S. B. 2009. *Turbulent Flows*. Cambridge, U.K.: Cambridge University Press.
Qingyan, C., J. Van der Kooi, and A. T. Meyers. 1988. Measurements and computations of ventilation efficiency and temperature efficiency in a ventilated room. *Energy Build.* 12(2): 85-99.
Shilo, E., M. Teitel, Y. Mahrer, and T. Boulard. 2004. Airflow patterns and heat fluxes in roof-ventilated multi-span greenhouse with insect-proof screens. *Agric. Forest Meteorol.* 122(1-2): 3-20.
Tanny, J., L. Haijun, and S. Cohen. 2006. Airflow characteristics, energy balance, and eddy covariance measurements in a banana screenhouse. *Agric. Forest Meteorol.* 139(1-2): 105-118.
Tanny, J., V. Haslavsky, and M. Teitel. 2008. Airflow and heat flux through the vertical opening of buoyancy-induced naturally ventilated enclosures. *Energy Build.* 40(4): 637-646.
Teitel, M., O. Liran, J. Tanny, and M. Barak. 2008. Wind-driven ventilation of a mono-span greenhouse with a rose crop and continuous screened side vents and its effect on flow patterns and microclimate. *Biosyst. Eng.* 101(1): 111-122.
Valera, D. L., A. J. Álvarez, and F .D. Molina-Aiz. 2006. Aerodynamic analysis of several insect-proof screens used in greenhouses. *Spanish J. Agric. Res.* 4(4): 273-279.
Valera, D. L., A. López, F. D. Molina-Aiz, and A. J. Álvarez. 2009. Estudio del flujo de aire y de la turbulencia en las aperturas de ventilación en invernaderos mediterráneos. In *Proc. V Congreso Nacional y II Congreso Ibérico de Agroingenería.* Lugo, Spain: Escola Politécnica Superior, Departamento de Ingeniería Agroforestal.
Wang, S., and T. Boulard. 2000. Predicting the microclimate in a naturally ventilated plastic house in a Mediterranean climate. *J. Agric. Eng. Res.* 75(1): 27-38.
Wang, S., and J. Deltour. 1997. Natural ventilation induced airflow patterns measured by an ultrasonic anemometer in Venlo-type greenhouse openings. *Agric. Eng. J.* 6(3-4): 185-196.
Wang, S., and J. Deltour. 1999. Lee-side ventilation-induced air movement in a large-scale multi-span greenhouse. *J. Agric. Eng. Res.* 74(1): 103-110.

NOMENCLATURE

A_p = coefficient obtained from the vertical profiles of air speed for roof vent
D_f = insect-proof screen thread density according to the manufacturer (threads cm^{-2})
D_h = thread diameter (μm)
D_i = diameter of the inside circumference of the pore (μm)
D_r = insect-proof screen thread density measurement (threads cm^{-2})
G = volumetric flow rate ($m^3\ s^{-1}$)
L_{px} = length of the pore in the direction of the warp (μm)
L_{py} = length of the pore in the direction of the weft (μm)
R = ventilation rate for greenhouse (h^{-1})
R_g = solar radiation ($W\ m^{-2}$)
RH = relative humidity (%)
S_p = average surface of the pore (mm^2)
T = temperature (°C)
V_L = lateral vent length
V_R = roof vent length
ΔT_{io} = inside to outside temperature difference (°C)
e = thickness (μm)
i = turbulence intensity
k = turbulence kinetic energy ($m^2\ s^{-2}$)
l = two-dimensional horizontal resultant of air velocity on the XY plane ($m\ s^{-1}$)
q = specific humidity of the air ($g\ g^{-1}$)
u = air velocity ($m\ s^{-1}$)
u' = fluctuating component ($m\ s^{-1}$)
$\bar{u}$ = time-mean value of air velocity ($m\ s^{-1}$)
Δt = time interval (s)

GREEK LETTERS

φ = insect-proof screen porosity (%)
σ = standard deviation of the air velocity ($m\ s^{-1}$)
θ = wind direction (degrees)
η_T = ventilation efficiency for temperature

SUBSCRIPTS

o = outside
i = inside
ov = air exiting through the vents
s = sonic anemometer
sc = corrected sonic anemometer
x = longitudinal component
y = transversal component
z = vertical component
j = measurement point
M = average value

SUPERSCRIPTS

n = normalized
* = corrected